www.sensorsportal.com

Sensors & Transducers

Blind Single-Image Super Resolution Reconstruction with Defocus Blur

Fengqing Qin, Lihong Zhu, Lilan Cao, Wanan Yang
Institute of Computer Science and Technology in Yibin University,
Yibin, 644000, China
E-mail: qinfengqing@163.com, yibinwuyu@qq.com, 66243190@qq.com, ywaly@126.com

Received: 4 January 2014 /Accepted: 7 March 2014 /Published: 30 April 2014

Abstract: A blind single-image super resolution method is proposed to enhance the spatial resolution of the image with defocus blur. Firstly, according to the low resolution imaging model, a framework of blind single-image super resolution reconstruction is presented. Secondly, utilizing Wiener filtering algorithm, the error-parameter curve of the defocus blurred image was generated, through which the defocus radius was estimated approximately and automatically. Thirdly, the super resolution image is gained by iterative back projection algorithm. Experimental results showed that the defocus PSF was estimated with high precision, and justified the fact that the defocus blur estimation takes a great effect in blind single-image super resolution reconstruction. *Copyright © 2014 IFSA Publishing, S. L.*

Keywords: Single-image, Blind, Defocus blur, Iterative back projection, Wiener filter.

1. Introduction

High resolution (HR) image can offer more information details, which is often required in many electronics imaging applications. Image super resolution (SR) reconstruction means to generate a higher resolution image from one or multiple low resolution (LR) images, which is an efficient way with lower cost than hardware method.

According to the number of the utilized LR images, image SR mainly includes multi-image SR [1-3] and single-image SR [4-6]. Multi-image SR refers to reconstruct a higher resolution image from multiple LR images of the same scene, which is mostly researched in recent years. The sub-pixel movement and the prior information of the LR imaging system are utilized to reconstruct a HR image. The precision of image registration algorithm plays an important part in multi-image SR reconstruction. In some conditions, multiple LR images of the same scene can not be acquired. HR image should be reconstructed from a single LR image. In resent years, approaches have changed the classical SR paradigm with multiples images, evolving towards the use of information from a single LR image [7].

In many practical applications, the image restoration problem is always blind, which means that the PSF is most likely unknown or is known within a set of parameters [8]. Blind image SR has always been a difficult and challenge problem, which hasn’t been well resolved yet. The foremost difficulty of blind de-blurring is rooted in the fact that the observed image is an incomplete convolution. The convolution relationship around the boundary is destroyed by the cut-off frequency, which makes it much more difficult to identify the blurring function.

In most images SR reconstruction algorithm, the more accurate the estimation of the LR imaging model is estimated, the better the quality of the reconstructed SR image will be achieved. However, in most of the current algorithms, the blur is assumed to be a known blur with given parameters, or the blur process is not considered at all in some algorithms, which does not meet the real imaging model of optical devices. Thus, the blind image SR reconstruction [9-10] problem arises naturally and is expressed as estimating a HR image and the PSF simultaneously, which is one advanced issue and challenge in image restoration.

In this paper, a framework of blind single-image SR reconstruction method with defocus blur is proposed. The defocus blur of the LR image is estimated through error parameter analysis method. The SR image is reconstructed through iterative back projection (IBP) algorithm.

2. Framework of Defocus Blurred Single-image SR Reconstruction

2.1. The LR Imaging Model

In the LR imaging model, the defocus blur, down-sampling and noise are considered, as shown in Fig. 1. The mathematical description of LR imaging model of single-image SR reconstruction may be expressed as follows:

$$Y=BDF+N, \tag{1}$$

where Y represents the LR image; B is the blur function; D is the down-sample process; N is the noise.

The real scene may be expressed as a high resolution (HR) image. Firstly, the HR image is blurred by convolving with a defocus point spread function (PSF). Secondly, the blurred image is down-sampled by a given integer factor. Here, the down-sampled image is gained by taking the neighborhood average gray value of the blurred image. Thirdly, the down-sampled is noised by adding white Gaussian noise to generate a LR image.

2.2. The Iterative Back Projection Algorithm

The main principle of iterative back projection (IBP) algorithm is addressed as follows. If the reconstructed super-resolution image is close to the original high-resolution image, the simulated output low-resolution images gained by the reconstructed super-resolution image under the low-resolution observation model will be consistent with the input low-resolution image of the system. Projecting the error onto the high-resolution image grid, with the convergence of the error, the corresponding super-resolution image will ultimately be got.

According to this idea, the process of the iterative back projection method may be shown in Fig. 2. Here, k is the iteration time; $\hat{f}$ is the estimated SR image; y is the observed LR image; $\hat{y}$ is the simulated LR images of $\hat{f}$ passed through the LR imaging model; B and D are the matrix forms of the defocus blur and down-sampling respectively; n is the system noise; B^{-1}, D^{-1} and n^{-1} denote the inverse operation of B, D and n; H^{BP} is the back projection operation; $\hat{y}-y$ is the difference of simulated LR image and the original LR image; λ is the gradient step.

According to this idea, the IBP algorithm may be expressed as follows:

$$\hat{f}_{k+1} = \hat{f}_k - \lambda H^{BP}(\hat{y}_k - y) \tag{2}$$

The initial value $\hat{f}_0$ is taken as the Bilinear interpolation image of the LR image. The iterative process is repeated until that the iteration number reaches the maximum iteration number, or that the relative error $\left\|\hat{f}_{k+1}-\hat{f}_k\right\|^2 / \left\|\hat{f}_k\right\|^2$ is below a given threshold value. After several iterations, with the convergence of the error, the super-resolution reconstructed image will be gained ultimately.

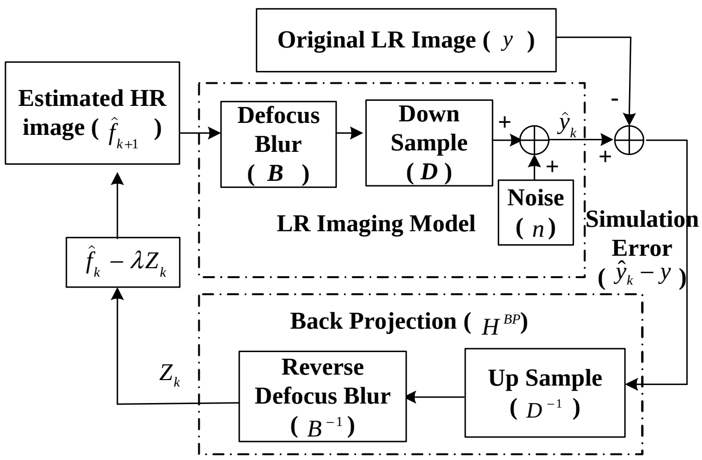

Fig. 1. Framework of blind defocus blurred single-image SR reconstruction.

2.3. Wiener Filter Algorithm

In Wiener filtering algorithm, both the blur function and the statistical character of system noise are considered. The noise is assumed to be a random process. The aim is to make the mean square error between the original image and the estimated image to be the least. According to this idea, the sketch map of Wiener filtering may be expressed in Fig. 2.

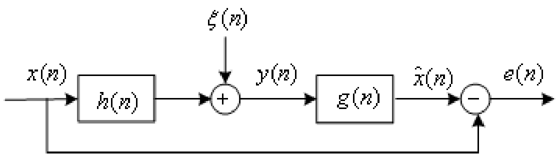

Fig. 2. The sketch map of Wiener filtering.

The observed low resolution image may be expressed as follows:

$$y(n)=\sum_{k=-\infty}^{\infty}x(n-k)h(k)+\xi(n)=x(n)*h(n)+\xi(n), \tag{3}$$

where * is the convolution operation; $x(n)$ is the original high resolution image; $\xi(n)$ is the Gaussian white noise with zero mean; $h(n)$ is the blur function, which can be presented by point spread function.

When the discrete Fourier transform (DFT) method is used to estimate the restored image, the Wiener filter may be expressed as follows:

$$X=\frac{H^{*}Y}{|H|^{2}+S_{nn}/S_{xx}} \tag{4}$$

where X, Y and H are the DFT of the real image (x), the blurred image (y) and the blur function (h) respectively; * denotes the conjugate operation; S_{nn} and S_{xx} denote the power spectrum of the noise and the real image. As it is usually very difficult to estimate S_{nn} and S_{xx}, the Wiener filter is usually approximated by the following formula:

$$X=\frac{H^{*}Y}{|H|^{2}+\Gamma}, \tag{5}$$

where Γ is the positive constant, which is often taken as an experience value.

3. Defocus Blur Estimation

3.1. Defocus Blur

Defocus blur refers to the image degradation caused by the incorrect focus of the optical system during the imaging process. Geometrical optic analysis shows that the point spread function (PSF) of defocus blur is a uniformly distributed circular facula. The defocus PSF may be expressed as following:

$$h(m,n)=\begin{cases}1/(\pi R^{2}) & m^{2}+n^{2}\le R^{2}\\ 0 & \text{others}\end{cases}, \tag{6}$$

where R is the defocus radius, which needs to be estimated.

3.2. Error-parameter Analysis

Error-parameter analysis method is utilized to estimate the parameter of defocus PSF. Wiener filtering method is used to generate the error-parameter curve.

Given a range of the defocus radius [R_{min}, R_{max}], the parameter (R) increases with a given increment. For each parameter, utilizing Wiener filtering image restoration method, a restored image may be gained, and the corresponding restoration error may be calculated. In this way, an error-parameter curve is generated at different defocus radius (R). By analyzing the relationship of this curve, the real defocus radius can be estimated approximately.

The defocus blur estimation criterion is as follows: when the parameter (R) changes from big to small, the slope of the error-parameter curve decreases evidently around the real parameter. Given a threshold of curve slope, the real defocus radius can be estimated automatically.

The description of this algorithm may be expressed as follows:

Step 1: Select a range of defocus radius [R_{min}, R_{max}], a researching number S. So, ΔR=(R_{max} - R_{min})/S;

Step 2: for i=1:S

Calculate the current parameter: $R_i = R_{\min} + (i-1)\Delta R$;

Calculate the current PSF: $h=1/R_i$;

Using Wiener filter, calculate the estimated image ($\hat{x}_i$);

Calculate the estimation error: $E_i=\|y-\hat{x}_i*h_i\|$

end

Step 3: Under different parameter (R), plot the error-parameter curve (E).

Step 4: Calculate the increment at different defocus radius on this curve from big to small. Once the increment is smaller than the threshold T_1, the defocus radius $\hat{R}$ of the defocus PSF is estimated.

4. Experiments

4.1. Simulated LR Image

Experiments are performed on simulated LR image to test the algorithm objectively and subjectively. The HR image 'lena.bmp' with size of

256×256 as shown in Fig. 3 is taken to simulate the real scene, which is passed through the LR imaging model as shown in Fig. 1 to simulate a LR image. Firstly, the HR image is convolved by a defocus PSF with radius (R_0) of 1.7. Secondly, the defocus blurred image is down-sampled by a factor of 2 in horizontal and vertical direction. Finally, Gaussian noise with standard deviation of 0.0001 is added. The generated LR image with size of 128×128 is shown in Fig. 4.

Fig. 3. The HR image.

Fig. 4. The simulated LR image.

4.2. Defocus PSF Estimation

When R_{min}=0.5, R_{max}=3, S=40, and the threshold of curve slope is taken as 0.01, using Wiener filtering image restoration algorithm, the restoration error (E) at different defocus radius (R) is calculated. The error-parameter curve of the blurred image is shown in Fig. 5.

From the error-parameter curve, we can see that when the defocus radius changes from big to small, the curve slope around the real defocus radius decreases obviously. Using the proposed defocus blur estimation algorithm, the estimated defocus radius ($\hat{R}$) is 1.75. The absolute estimation error is 0.05, and the relative estimation error is: (1.75-1.7)/1.7=0.0294. The estimated defocus PSF is shown in Fig. 6.

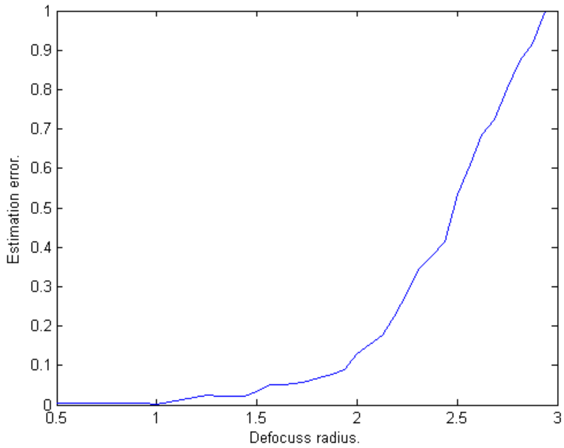

Fig. 5. The error parameter curve.

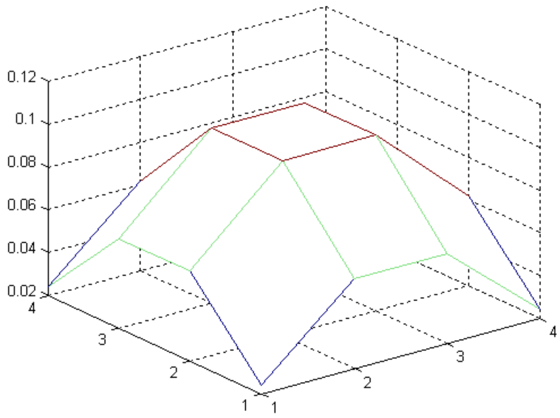

Fig. 6. The estimated defocus PSF.

4.3. Super Resolution Reconstruction

When the estimated defocus radius is 1.75, utilizing IBP algorithm, blind super resolution is performed on the simulated LR image as shown in Fig. 4. When the maximum iteration number is taken as 30, and the relative iteration error is 1×10^{-6}, the convergent curve of the IBP algorithm is shown in Fig. 7.

The reconstructed SR image is shown in Fig. 8. The peak-to-noise ratio (PSNR) of the SR reconstructed image relative to the HR image as shown in Fig. 3 is 34.7878 *dB*. The Bilinear interpolated image of the LR image by a factor of 2 is shown in Fig. 9, and the PSNR is 32.7351 *dB*.

4.4. Influence of Defocus Blur Estimation

To test the effect of defocus blur estimation on the quality of blind single-image SR reconstruction, SR reconstruction is performed on different estimated defocus radiuses.

When the estimated is taken from 0.5 to 4 with an increment of 0.1, the corresponding PSNRs of the reconstructed SR images are shown in Fig. 10. From Fig. 10, we can see that the PSNRs of the SR reconstructed images around the real defocus radius are higher than other cases. When the estimated defocus radiuses are far away (for example, more than 3) from the real value, the PSNRs of the SR reconstructed images is even lower than Bilinear interpolation algorithm.

When the estimated defocus radius is taken as 0.5, 2, 3 and 4 respectively, the corresponding SR reconstructed images are shown in Fig. 11(a)-Fig. 11(d).

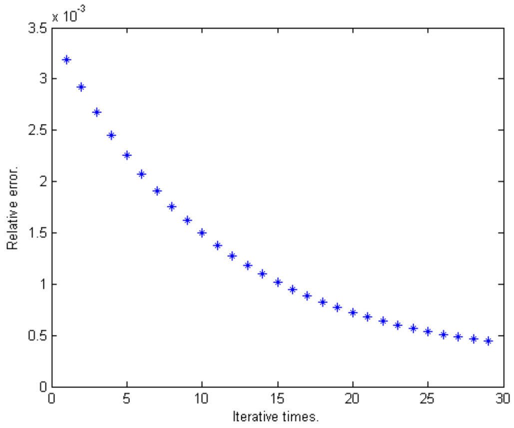

Fig.7. The convergent curve of the IBP algorithm.

Fig. 8. The SR reconstructed image.

Fig. 9. The Bilinear interpolated image.

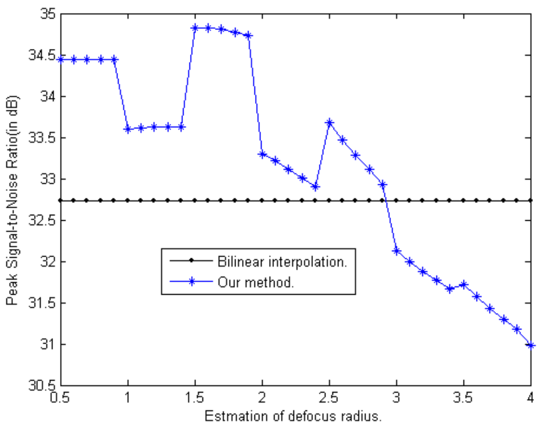

Fig. 10. The PSNRs of the SR reconstructed images at different estimated defocus radius.

(a) When the estimated defocus radius is 0.5

(b) When the estimated defocus radius is 2.

(c) When the estimated defocus radius is 3

(d) When the estimated defocus radius is 4.

Fig. 11. The SR reconstructed images at different estimated defocus radius.

By comparing Fig. 8, Fig. 9 and Fig. 11, the corresponding PSNRs of the images are shown in Table 1.

Table 1. The PSNRs of different methods.

Figures	PSNRs (in *dB*)
Fig. 7	34.7878
Fig. 8	32.7351
Fig. 10(a)	34.4399
Fig. 10(b)	33.2954
Fig. 10(c)	32.1277
Fig. 10(d)	30.9765

From the experimental results, we can see that the SR reconstructed image around the real defocus blur has higher PSNR and better visual effect. When the estimated defocus radius is smaller than the real value, the SR reconstructed image is vague. When the estimated defocus radius is larger than the real value, the SR reconstructed image has obvious ringing effect.

5. Conclusions

A framework of blind defocus blurred single-image SR reconstruction method is proposed. The defocus blur, down-sampling and noise are considered in the LR imaging model. The defocus blur is estimated through parameter analysis method gained by Wiener filter algorithm. The SR image is reconstructed through IBP algorithm. The influence of defocus blur estimation on SR reconstructed image is justified in and experimental way. It can also be extensively used to handle other types of blur.

Acknowledgements

This paper is supported by the National Nature Science Foundation of China (Grant No. 61202195, 61202196), the Sichuan Provincial Education Department project (Grant No. 11ZA174, 11ZA223, 11ZA224), the Application Fundamental Research Project of Sichuan Provincial Scientific and Technology Department (Grant No. 2011JY0139), the key project of Yibin Science and Technology Bureau (Grant No. 2011SF016, 2013ZSF009).

References

[1]. D. C. Garcia, Super resolution for multiview images using depth information, *IEEE Transactions on Circuits and System for Video Technology*, Vol. 22, Issue 9, 2013, pp. 1249-1256.

[2]. L. Zhang, Q. Q. Yuan, H. F. Shen, and P. X. Li, Multiframe image super-resolution adapted with local spatial information, *Journal of Optical Society of America A – Optics Image Science and Vision*, Vol. 28, No. 3, 2011, pp. 381-390.

[3]. A. Giannoula, Classification-based adaptive filtering for multiframe blind image restoration, *IEEE Transactions on Image Processing*, Vol. 20, Issue 2, 2011, pp. 382-390.

[4]. S. Y. Yang, M. Wang, Y. G. Chen, and Y. X. Sun, Single-image super-resolution Reconstruction via learned geometric dictionaries and clusters sparse coding, *IEEE Transactions on Image Processing*, Vol. 21, Issue 9, 2012, pp. 4016-4028.

[5]. K. I. Kim, and Y. Kwon, Single-image super-resolution using sparse regression and natural image prior, *IEEE Transactions on Pattern Analysis and Machine Intelligence*, Vol. 32, Issue 6, 2010, pp. 1127-1133.

[6]. D. Chris, Single image super-resolution using self-examples and texture synthesis, *Signal Image and Video Processing SIViP*, Vol. 5, 2011, pp. 343-352.

[7]. A. Rueda, N. Malpica, and E. Romero, Single-image super resolution of brain MR images using overcomplete dictionaries, *Medical Image Analysis*, Vol. 17, Issue 7, 2013, pp. 113-132.

[8]. M. Y. Zou, Deconvolution and signal recovery, *Defense Industry Publishing*, Beijing, 2004.

[9]. F. Q. Qin, L. H. Zhu, L. L. Cao, Blind single-image super-resolution reconstruction based on motion blur, *Advanced Materials Research*, Vol. 225-226, 2011, pp. 895-899.

[10]. J. P. Qiao, J. Liu, and Y.-W. Cheng, Joint blind super-resolution and shadow removing, *IEICE Transactions on Information & Systems*, Vol. E90-D, No. 12, 2007, pp. 2060-2069.